

Supplement to Diener et al. ‘Acceleration of dynamic ice loss in Antarctica from satellite gravimetry’

GRACE/GRACE-FO corrections

We use Stokes potential coefficients C_{jm} up to degree, j , and order, m , 60 and apply the following common corrections to the Level-2 data: 1) Insertion of degree-1 ($j = 1$) coefficients – which are not recovered by GRACE/GRACE-FO – provided by the SDS based on (Sun et al., 2016), an improvement to the estimation method originally proposed by (Swenson et al., 2008). These data are available as *GRACE Technical Note 13* from <https://podaac-tools.jpl.nasa.gov/drive/files/GeodeticsGravity/gracefo/docs/> for each SDS data set. 2) Replacement of highly uncertain C_{20} coefficients from GRACE/GRACE-FO by more accurate estimates from Satellite Laser Ranging (SLR) (Cheng et al., 2013), accessible as *GRACE Technical Note 14* from https://podaac-tools.jpl.nasa.gov/drive/files/GeodeticsGravity/gracefo/docs/TN-14_C30_C20_GSFC_SLR.txt .

Note that although the replacement of C_{30} coefficients is recommended by the GRACE/GRACE-FO SDS centers for solutions starting August 2016, this issue is still under discussion from the user point of view since it introduces a discontinuity in the time series between months with nominal and anomalous GRACE/GRACE-FO accelerometer performance (Bandikova et al., 2019; Loomis et al., 2020). In this study, we do not adopt this

Page 1

procedure.

The corrections for glacial-isostatic adjustment (GIA) are applied starting spherical harmonic degree $j = 2$, as degree-1 coefficients inserted according to (Sun et al., 2016) already reflect only surface-mass changes without GIA (corrected with ICE-6G_D; (Peltier et al., 2015)). As our processing is rather insensitive to the low-degree coefficients of GRACE/GRACE-FO (due to masking and weighting of the coefficients), the uncertainty of the mass trend for Antarctica introduced by uncertainties in the degree-1 coefficients due to the GIA correction is $< 0.1 \text{ Gt yr}^{-1}$.

Details on the GIA corrections are provided in Supplementary Figure 3. For the Amundsen Sea Embayment region, observed bedrock uplift and numerical modelling indicate a non-linear GIA (Barletta et al., 2018), which would influence the acceleration estimates derived from GRACE/GRACE-FO. However, due to inconsistency with the adopted GIA estimates, and unknown uncertainties provided with the inferred acceleration of GIA, we limit the GIA correction to the linear trends in the GRACE/GRACE-FO data.

GRACE/GRACE-FO solution combination

To reduce the noise level of the solutions and mitigate the impact of possible outliers (Jean et al., 2018), we estimate 191 combined GRACE/GRACE-FO monthly solutions (AV RL06). This combination is achieved by coefficient-wise weighting of the Stokes potential coefficients C_{jm} from SDS centers ($N_{sol} = 3$) for each time t , according to $C_{jm}^{AV,t} =$

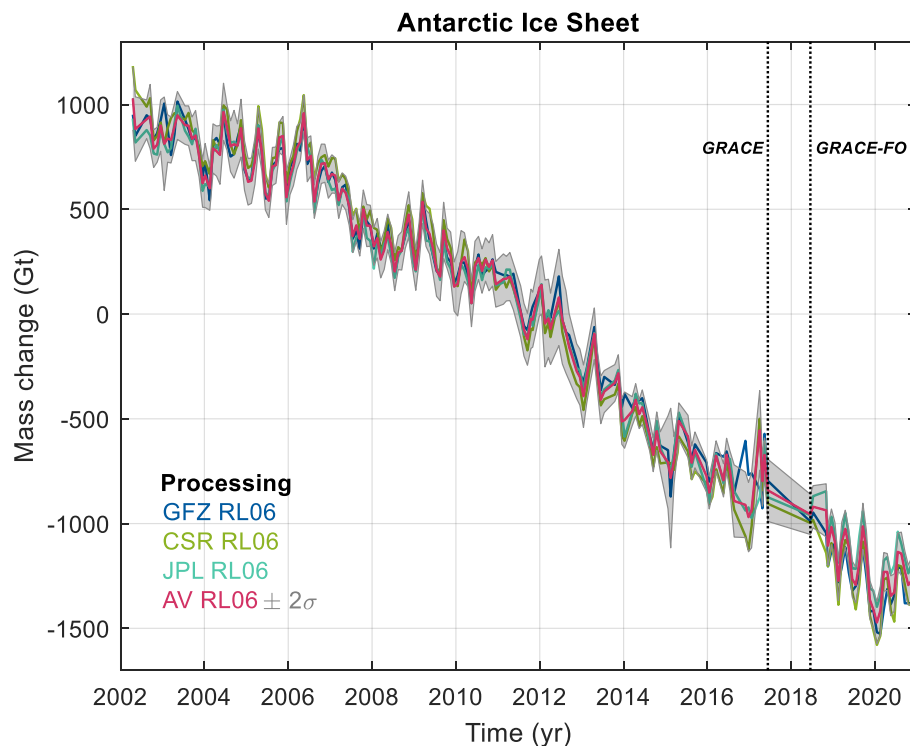
$\sum_{n=1}^{N_{sol}} (w_{jm}^{n,t} C_{jm}^{n,t}) / \sum_{n=1}^{N_{sol}} w_{jm}^{n,t}$, where $w_{jm}^{n,t}$ represent weights corresponding to the inverse of the squared variance of the calibrated uncertainty of each coefficient, $\hat{\sigma}_{jm}^{n,t-2}$. Formal uncertainties provided with the GRACE/GRACE-FO coefficients result from different estimation procedures that prevent their direct use as quantitative weights. Therefore, we calibrate the uncertainties based on the noise level of each solution as follows; we estimate the temporal residual, $C_{jm}^{Res.}$ after subtracting bias, trend, annual, semiannual and temporal variations longer than four months (using a moving average filter) from the GRACE/GRACE-FO coefficients' time series. We then determine the degree power in the noise-dominated spectral range ($j_{min} = 40$ to $j_{max} = 60$) according to $\sum_{j=j_{min}}^{j_{max}} \sum_{m=-j}^j (C_{jm}^{Res.})^2$, which is representative of the noise level in each solution. The formal uncertainties provided with the SDS centers are then calibrated by a single scaling factor to match the degree power of the residual estimated for GRACE/GRACE-FO coefficients, yielding $\hat{\sigma}_{jm}^n$. This approach adopts the error structure from the formal uncertainties with the error magnitude estimated from the residual.

We carry out the combination on detrended data, as the differences in the trends appear to be systematic and arising from different processing choices of the SDS centers (Supplementary Figure 1). Therefore, the monthly weights derived from coefficients beyond degree and order 40 are not representative for the relative uncertainty of the trends. Applying these weights to the different temporal linear signals would introduce artificial monthly temporal variability of about 1-2 Gt. Therefore, we remove the trends before combination and

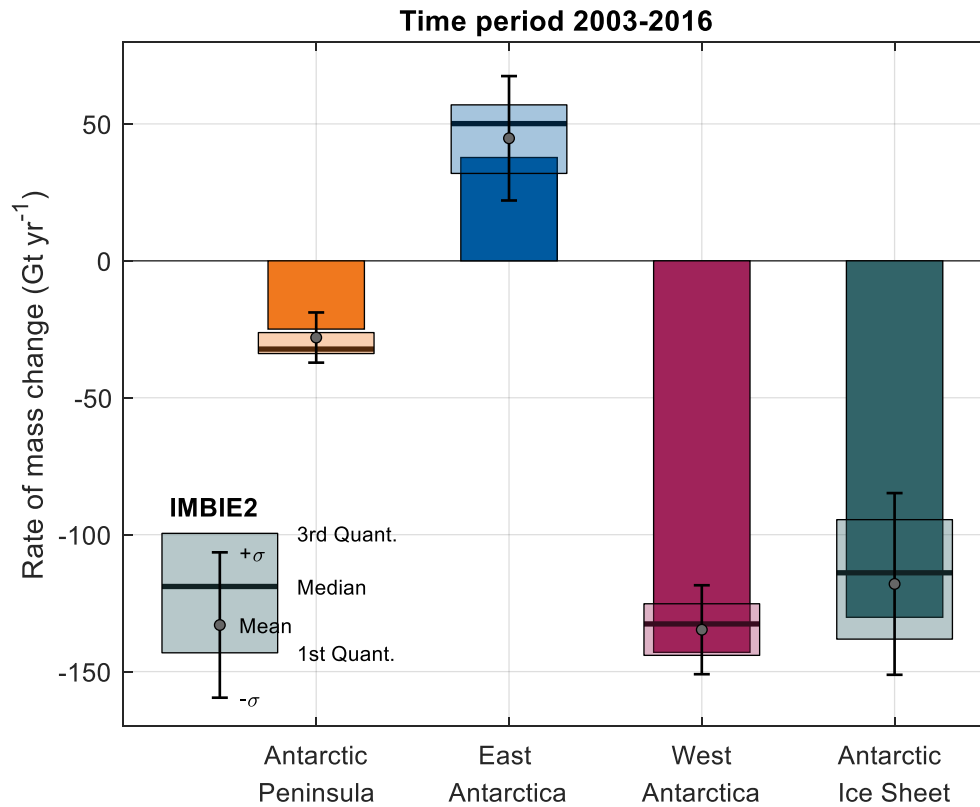
restore them, assuming equal weights for each SDS center, in the combined solution, C_{jm}^{AV} .

The mass change for the Antarctic Ice Sheet for the SDS solutions GFZ RL06, CSR RL06 and JPL RL06, as well as their combination AV RL06 are shown in Supplementary Figure 1, and their respective uncertainties are shown in Supplementary Figure 4.

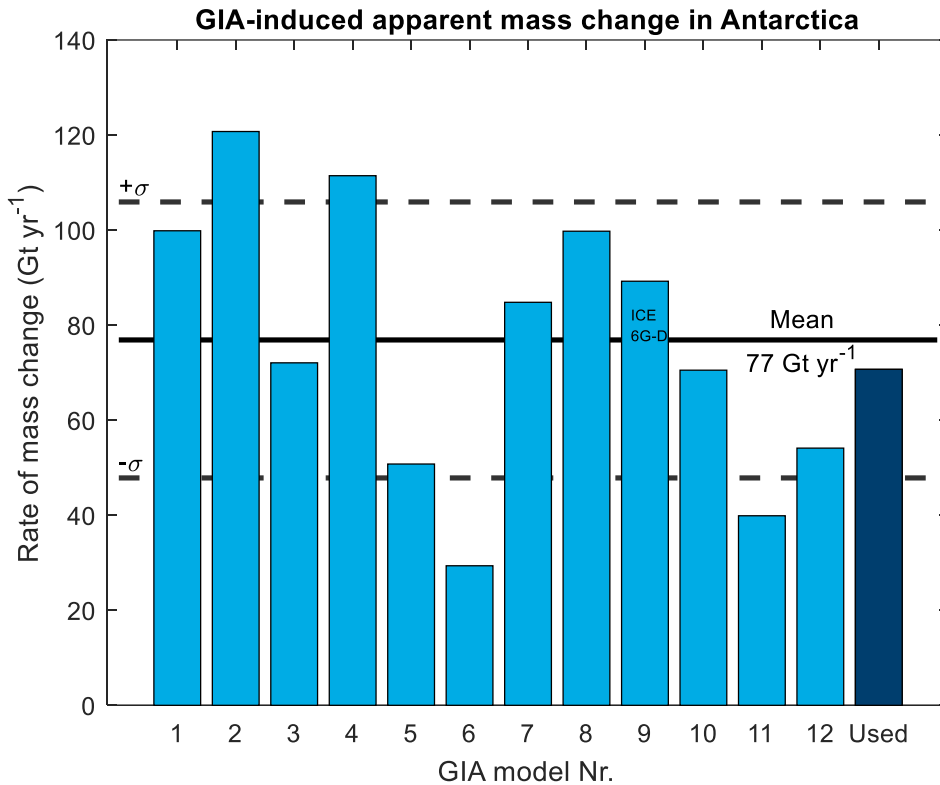
Supplementary Figures



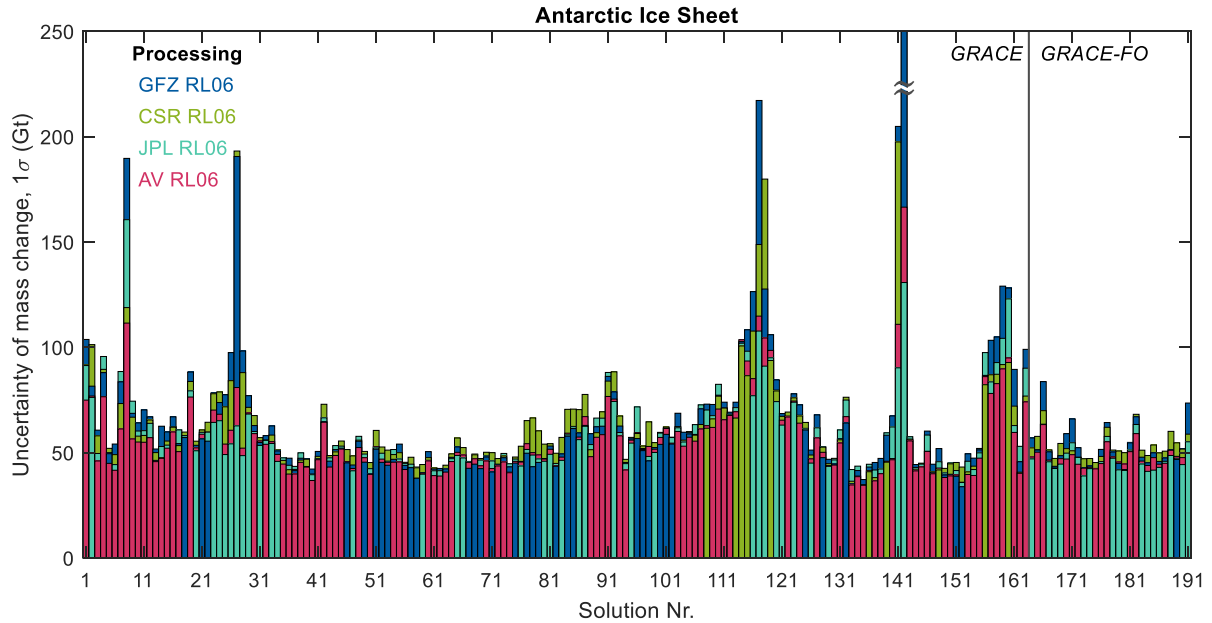
Supplementary Figure 1. Time series of Antarctic ice mass change from different data sets of monthly GRACE/GRACE-FO gravity field solutions. Shown are GRACE/GRACE-FO time series for 191 monthly solutions of release 6 (RL06) of the SDS processing centers GFZ, CSR and JPL, as well as the combined solution (AV RL06) derived for this paper, along with the estimated uncertainty (2σ) shown in Supplementary Figure 3. Typically, the uncertainty estimated for AV RL06 encompasses the spread exhibited by all solutions. Exceptions are monthly solutions at the end of the GRACE mission (November 2016 to June 2017, excluding April 2017), which are of poor quality due to the loss of the accelerometer on the GRACE-B satellite in October 2016, requiring modified solution procedures (Bandikova et al., 2019).



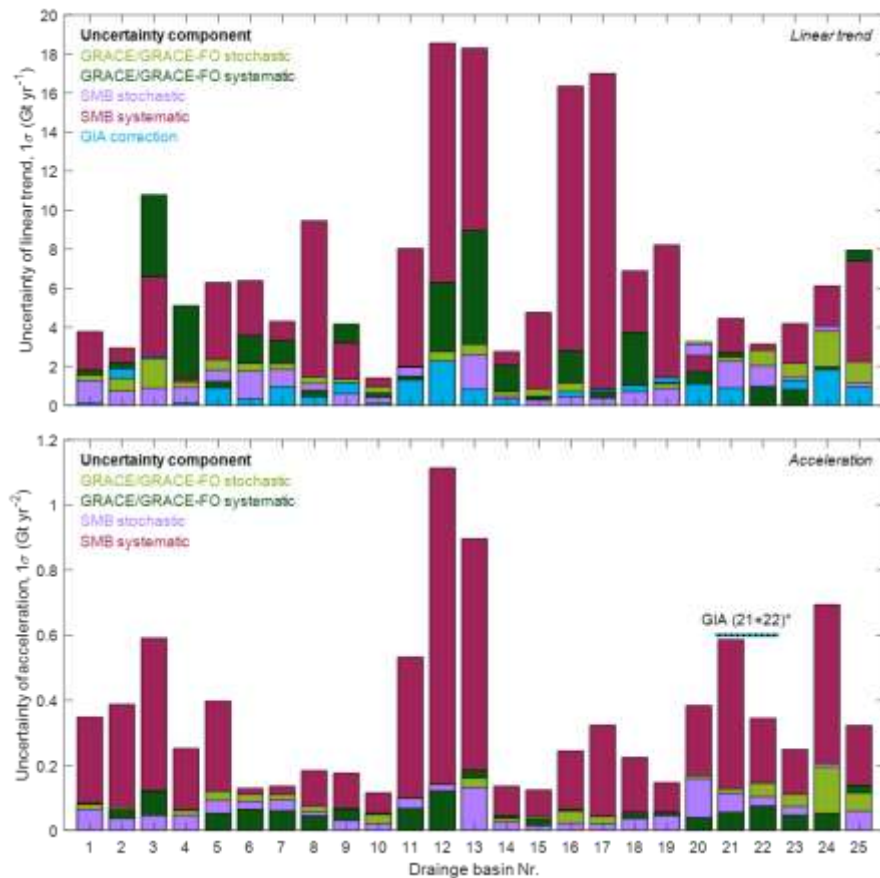
Supplementary Figure 2. Mass balance estimates from GRACE for Antarctica obtained in this study (opaque bars) compared with the estimates used in the IMBIE2 (Shepherd et al., 2018) estimates for the consistent time interval 2003 to 2016 (half-transparent boxes and circles with error bars). The boxes represent estimates of the IMBIE2 ensemble (14 members) indicate median (black horizontal line), the first and third quantile (half-transparent box), as well as the mean (circle) and $1-\sigma$ uncertainties (error bars). The plot shows that the estimates used in this study lies within the range of 50% of the IMBIE2 estimates, with the exception of the Antarctic Peninsula, which are slightly lower.



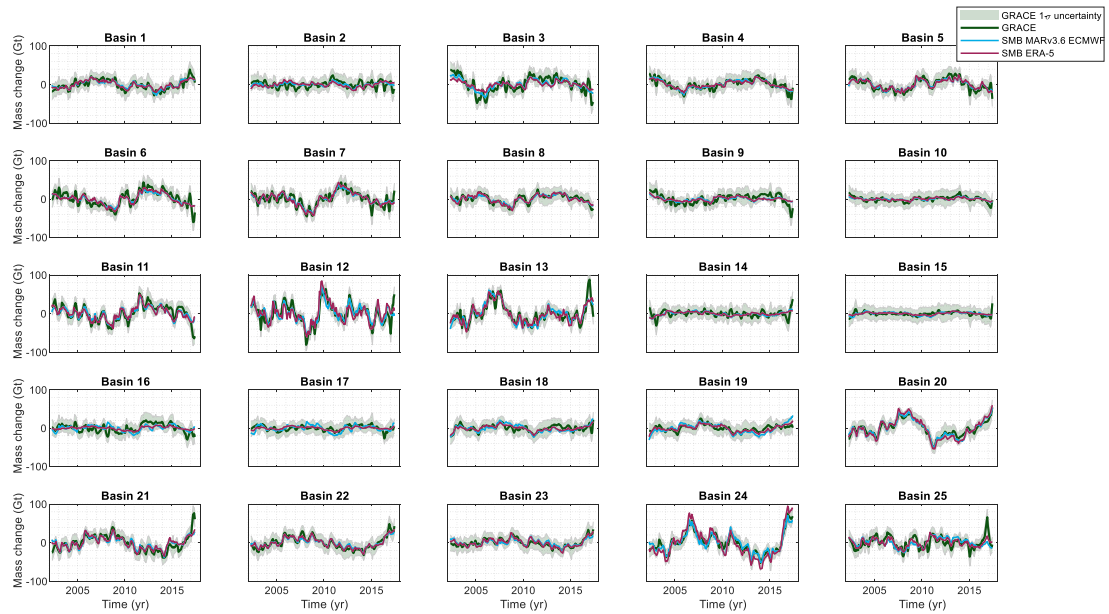
Supplementary Figure 3. Rate of apparent ice-mass change induced by glacial-isostatic adjustment (GIA) in Antarctica. Shown are 13 models; Model Nr. 9 is the commonly used ICE-6G (Peltier et al., 2015) (89 Gt yr⁻¹), “Used” represents the model applied in this study (71 Gt yr⁻¹), consisting of the average of model 3 (IJ05 R2; (Ivins et al., 2013), 5 (AGE1; (Sasgen et al., 2013)) and 9 (ICE-6G_D (Peltier et al., 2015))). The remaining models are anonymized, but listed in the GIA impact analysis of IMBIE2 (Shepherd et al., 2018). Note that the apparent mass change is estimated using an averaging Kernel over Antarctica including a 200 km buffer zone, applied to the spherical harmonic degree and order 2 to 60 of the GIA model. The effective value of the correction depends on the user’s processing scheme for estimating ice mass balances.



Supplementary Figure 4. Empirical uncertainty (1σ) of GRACE/GRACE-FO monthly mass changes of the Antarctic Ice Sheet. Shown are monthly uncertainty estimates for 191 monthly solutions of release 6 (RL06) the SDS processing centers GFZ, CSR and JPL, as well as the combined solution (AV RL06) used in this paper. The mean of the 1σ -uncertainties of the solutions are ± 65 Gt (GFZ RL06), ± 64 Gt (CSR RL06), ± 57 Gt (JPL RL06) and ± 55 Gt (AV RL06). The estimated noise level of the combined solution lies below or is very close to the lowest noise level of any of the entering solutions, particularly improving epochs with elevated noise characteristics (e.g. solution number 142 for GFZ RL06 and CSR RL06 with an uncertainty of ± 615 Gt and ± 645 Gt, respectively). Note that the combination minimizes the noise level in the global combined solutions, which may not yield to a minimum noise level combination at this regional scale.

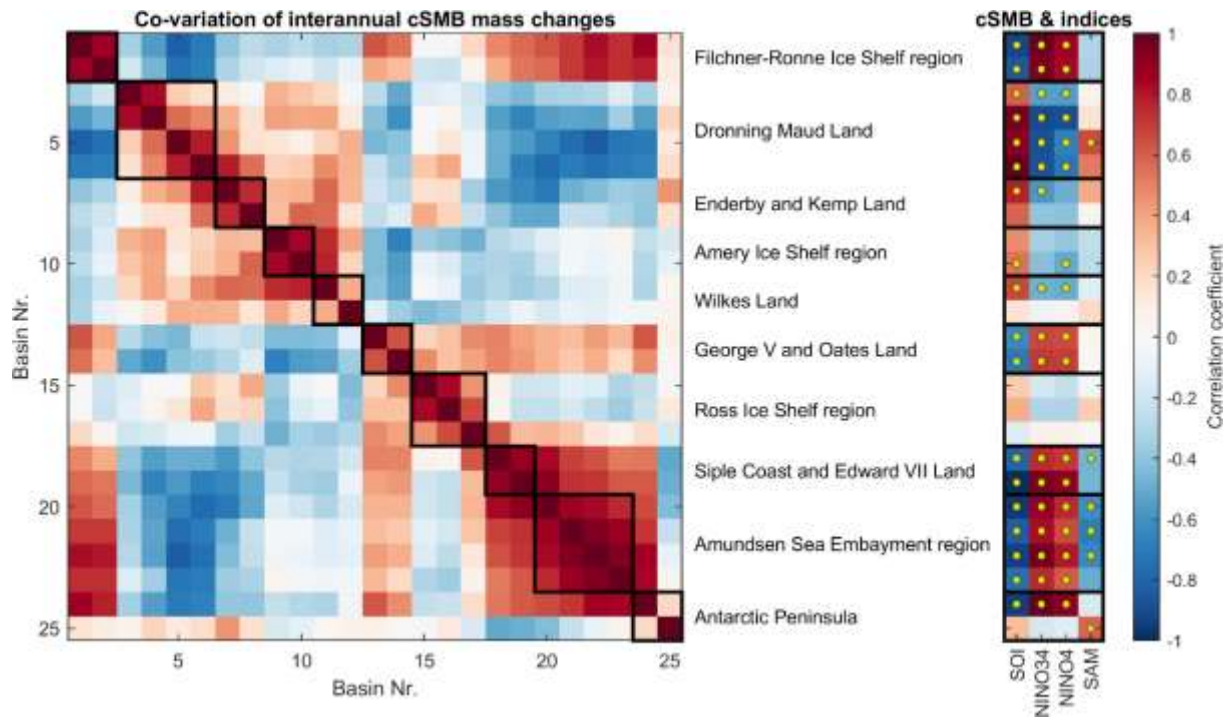


Supplementary Figure 5. Uncertainty (1σ) components of the (A) linear trend and (B) acceleration of mass change from GRACE/GRACE-FO and cumulative SMB for 25 drainage basins in Antarctica. The uncertainties are separated into propagated monthly uncertainties ('stochastic'), as well as differences of the temporal component between data sets ('systematic'). For the linear trend we include the uncertainty introduced by the GIA correction. For the acceleration, we indicate the magnitude (not the uncertainty) of a possible non-linear GIA response (*) suggested by (Barletta et al., 2018). The largest uncertainty associated with estimating discharge acceleration is caused by systematic differences between the SMB estimates.



Supplementary Figure 6. Interannual mass balance changes for the Antarctic Ice

Sheet between April 2002 and June 2017. Shown are monthly mass changes without trends and accelerations for 25 drainage basins obtained from GRACE $M(t)$ (green, with pink $1-\sigma$ error shading) and cumulative SMB estimates, $SMB(t)$ based on output of MARv3.6 forced by ECMWF ERA-Interim (light blue) and ERA-5 (purple), the latter being used in this paper.



Supplementary Figure 7. (A) Correlation of interannual cumulative SMB mass changes, $SMB(t)$, between 25 drainage basins in Antarctica. Groups of co-varying behaviour related to a common atmospheric forcing are used to aggregate the 25 basins into ten regions. In addition, we ensure regions of similar size and largely retaining geographic attributions; for example, we group basin 24 and 25, while basin 24 shows stronger correlation with the Amundsen Sea Embayment region. (B) Correlation of interannual $SMB(t)$ in the 25 drainage basins with the cumulative atmospheric indices, SOI, NIÑO3.4/4 and SAM.

Supplementary Table 1

Results of the Student's t -test at a significance level of 5 % for accelerations of the cumulative discharge for the 25 drainage basins. Significance is tested assuming stochastic and systematic uncertainties shown in Supplementary Figure 5 (Full), as well as formal uncertainties obtained from least-squares adjustment (Regr.). In addition, the table shows the root-mean-squared (RMS) estimate of the data before (Pre-fit) and after the fit of the acceleration terms (Post-fit). The value of one indicates the rejection of the null hypothesis that the acceleration parameter is zero.

Basin Nr.	Significance (t -test)		RMS (Gt)	
	Full	Regr.	Pre-fit	Post-fit
1	0	1	13.7	13.1
2	0	1	14.5	12.0
3	0	1	19.5	18.5
4	0	1	8.1	6.4
5	0	0	7.3	7.1
6	0	1	9.1	8.7
7	0	1	8.8	8.4
8	0	0	8.7	8.6
9	0	0	11.0	11.0
10	1	1	10.2	8.6
11	0	0	10.6	10.6
12	0	1	17.0	16.5
13	0	1	20.2	16.0
14	0	1	6.2	5.9
15	0	0	7.6	7.6
16	0	0	11.1	10.9
17	0	1	8.1	8.0
18	1	1	11.5	9.6
19	0	0	14.1	14.1
20	1	1	21.0	13.3
21	1	1	21.9	14.6
22	1	1	27.5	19.2
23	1	1	10.8	9.3
24	0	1	21.3	15.5
25	1	1	24.4	20.2

Supplementary Table 2

Same as Supplementary Table 1, but for the basins grouped into ten regions.

Region	Significance (<i>t</i> -test)		RMS (Gt)	
	Full	Regr.	Pre-fit	Post-fit
Antarctic Peninsula	0	0	21.4	21.4
Amundsen Sea Embayment region	1	1	73.2	45.2
Siple Coast and Edward VII Land	1	1	21.4	20.2
Ross Ice Shelf region	0	0	21.7	21.5
George V and Oates Land	0	1	20.5	17.6
Wilkes Land	0	0	22.4	22.0
Amery Ice Shelf region	1	1	18.0	17.3
Enderby and Kemp Land	0	1	10.7	10.1
Dronning Maud Land	0	1	34.2	30.6
Filchner-Ronne Ice Shelf region	1	1	22.5	19.0

References

- Bandikova, T., McCullough, C., Kruizinga, G. L., Save, H., and Christophe, B. (2019). GRACE accelerometer data transplant. *Adv. Space Res.* 64, 623–644. doi:10.1016/j.asr.2019.05.021.
- Barletta, V. R., Bevis, M., Smith, B. E., Wilson, T., Brown, A., Bordoni, A., et al. (2018). Observed rapid bedrock uplift in Amundsen Sea Embayment promotes ice-sheet stability. *Science* 360, 1335–1339. doi:10.1126/science.aao1447.
- Cheng, M., Tapley, B. D., and Ries, J. C. (2013). Deceleration in the Earth’s oblateness: J2 variations. *J. Geophys. Res. Solid Earth* 118, 740–747. doi:10.1002/jgrb.50058.
- Ivins, E. R., James, T. S., Wahr, J., O. Schrama, E. J., Landerer, F. W., and Simon, K. M. (2013). Antarctic contribution to sea level rise observed by GRACE with improved GIA correction. *J. Geophys. Res. Solid Earth* 118, 3126–3141.
- Jean, Y., Meyer, U., and Jäggi, A. (2018). Combination of GRACE monthly gravity field solutions from different processing strategies. *J. Geod.* 92, 1313–1328. doi:10.1007/s00190-018-1123-5.
- Loomis, B. D., Rachlin, K. E., Wiese, D. N., Landerer, F. W., and Luthcke, S. B. (2020). Replacing GRACE/GRACE-FO With Satellite Laser Ranging: Impacts on Antarctic Ice Sheet Mass Change. *Geophys. Res. Lett.* 47. doi:10.1029/2019GL085488.

- Peltier, W. R., Argus, D. F., and Drummond, R. (2015). Space geodesy constrains ice age terminal deglaciation: The global ICE-6G_C (VM5a) model. *J. Geophys. Res. Solid Earth* 120, 450–487. doi:10.1002/2014JB011176.
- Sasgen, I., Konrad, H., Ivins, E. R., Van den Broeke, M. R., Bamber, J. L., Martinec, Z., et al. (2013). Antarctic ice-mass balance 2003 to 2012: regional reanalysis of GRACE satellite gravimetry measurements with improved estimate of glacial-isostatic adjustment based on GPS uplift rates. *The Cryosphere* 7, 1499–1512.
- Shepherd, A., Ivins, E., Rignot, E., Smith, B., van den Broeke, M., Velicogna, I., et al. (2018). Mass balance of the Antarctic Ice Sheet from 1992 to 2017. *Nature* 556, 219–222.
- Sun, Y., Riva, R., and Ditmar, P. (2016). Optimizing estimates of annual variations and trends in geocenter motion and J_2 from a combination of GRACE data and geophysical models. *J. Geophys. Res. Solid Earth* 121, 8352–8370. doi:10.1002/2016JB013073.
- Swenson, S., Chambers, D., and Wahr, J. (2008). Estimating geocenter variations from a combination of GRACE and ocean model output. *J. Geophys. Res. Solid Earth* 113. doi:10.1029/2007JB005338.